RESEARCH ARTICLE

High Sensitivity and Specificity in Healthcare: Design and Validation of a Novel SiNW-FET Biosensor for Viral Detection

AHMED HADDED[1], MOSSAAD BEN AYED[1,2], AND SHAYA ABDULLAH ALSHAYA[ID]3
[1]Computer and Embedded System Laboratory, National Engineering School of Sfax, Sfax University, Sfax 3038, Tunisia
[2]Department of Electronic Industrial, National Engineering School of Sousse, Sousse University, Sousse 4054, Tunisia
[3]Department of Computer Science, Faculty of Sciences and Humanities Sciences, Majmaah University, Al Majma'ah 11952, Saudi Arabia

Corresponding author: Mossaad Ben Ayed (mossaad.benayed@eniso.u-sousse.tn)

ABSTRACT Impedance biosensing offers a highly sensitive and non-invasive method for detecting biomolecules and monitoring cellular activities, which is crucial for timely diagnosis and management of viral infections. Traditional methods, although effective, often involve costly and cumbersome equipment and require frequent hospital visits, making them less practical for continuous monitoring. This study introduces a novel biosensor based on SiNW-FET coupled with an advanced preamplifier designed to detect viruses through impedance changes caused by the interaction of antibodies and antigens. Utilizing COMSOL/MATLAB simulations, this research accurately models the sensor's response to electrode functionalization with antibodies, and evaluates how nanoscale adjustments in electrode size and spacing can enhance biosensing capabilities. The proposed system promises continuous patient monitoring, alerting healthcare providers to critical changes that might indicate viral infections or significant shifts in cellular behavior. The performance of the sensor, validated through detailed simulations, demonstrates its potential as an effective tool for healthcare, ensuring timely interventions and improved patient outcomes. The proposed sensor design achieved an accuracy of approximately 92%, a sensitivity of about 85%, and a specificity of roughly 99%, demonstrating its high effectiveness in detecting viral infections and ensuring accurate monitoring. The sensor highlighted its potential as an effective tool for real-time, non-invasive healthcare monitoring.

INDEX TERMS Biosensor, impedance, nanoscale, simulation, virus detection.

I. INTRODUCTION

Biosensors are utilized across a broad range of applications, from detecting cells [1] and toxins [2] to monitoring diseases at their early stages [3], [4]. These devices incorporate various mechanical, optical, and electrochemical principles in their design [5], [6], with electrochemical methods being particularly valued for their speed and cost-efficiency in detection [7]. These biosensors measure changes in electrical properties that occur when biological elements such as cells, proteins, nucleic acids, and other biomarkers are present. Specifically, they monitor alterations in the electric field at

The associate editor coordinating the review of this manuscript and approving it for publication was Paolo Crippa [ID].

the electrode surface or in the spaces between electrodes when these elements interact with or are near the sensor [8].

In practice, electrodes within the sensor detect and analyze cells or biomarkers through multi-frequency impedance-based characterization, leveraging the dielectric properties like capacitance and conductivity of these entities. For instance, this technique is capable of identifying variations in cell physiology, size, or morphology over time [9], offering significant improvements over traditional methods by enabling real-time, label-free, non-invasive analyses that are easy to integrate and suitable for high-throughput screening [10].

Sensors are designed to identify analytes that have differing dielectric constants from their surrounding medium,

based on the spacing between electrodes and the selective layers of bio- or chemical-sensitive materials applied to them. In resistive chemical sensors, a conductive thin layer envelops the electrodes. Variations in the concentration of the analyte alter the resistance within this thin sensing layer. Models such as Randle's model are used to understand the electrical interactions among the electrodes, sensing layers, target cells, and the surrounding solution [11].

Impedance changes due to cell growth are utilized to track cell behavior alterations. These changes are depicted through an equivalent circuit model consisting of resistors and capacitors that represent both the cell culture media and the cells themselves. Historically, detecting these impedance changes required the use of costly and bulky impedance analyzers. Research has also focused on optimizing the dimensions of sensors to enhance their sensing capabilities [12].

Previous studies have explored impedance-based methods for applications such as cell counting, assessing the impact of gold nanoparticles on sensors, modeling cell growth, and detecting bacteria like E. coli. Despite the widespread use of antibody-antigen interactions in impedance biosensing, the need for timely viral infection diagnostics remains critical in healthcare. Some patients require ongoing monitoring or frequent testing, which can be both complex and expensive. Consequently, there is a national effort to minimize unnecessary medical visits, underscoring the need for a home healthcare device that continually monitors and detects changes in a patient's health, prompting visits to healthcare facilities only when absolutely necessary.

This research introduces a novel sensor and healthcare monitoring system that has been developed and simulated to detect viruses by monitoring impedance changes caused by the binding of antibodies and antigens. The study is divided into two primary sections. First, COMSOL is used to validate the internal design of the sensor and MATLAB for the complete architecture including the operational amplifier. The proposed model demonstrates the feasibility of using impedance changes as indicators of changes in human cell behavior, showing a correlation between impedance variations and cellular alterations, with expected increases in impedance during the electrode functionalization with antibodies and subsequent antigen binding. This healthcare monitoring system continuously tracks a patient's condition, alerting to any impedance changes that signify virus detection or changes in cellular activity.

The paper is organized as follows: Section II provides a comprehensive literature review on biosensors, including a comparative analysis that highlights the advantages and disadvantages of each biosensor model. Section III focuses on the overall architecture of the sensor, with a particular emphasis on the design of the amplifier. Section IV offers an in-depth examination of the internal design of the SiNW-FET biosensor. Subsequently, the results and discussion section elaborates on the simulation outcomes, assessing the sensor's behavior and the overall performance of the proposed architecture. The paper concludes with a final section summarizing the key findings and implications of the study.

II. LITERATURE REVIEW

Biosensors are analytical tools that convert biological responses into quantifiable signals. These devices typically incorporate biological materials such as enzymes, tissues, microorganisms, antibodies, cell receptors, or biomimetic components immobilized on a transducer. The interaction between the biological material and the analyte in a solution triggers a biochemical response, which the transducer then converts into a measurable signal that a digital module can detect [13], [14].

Various transducing systems like electrochemical, optical, and piezoelectric are essential in the design of biosensors. Electrochemical biosensors use potentiometric, amperometric, or impedimetric principles to monitor changes in charge distribution on the transducer surface [15], [16], [17], [18]. Optical biosensors provide multiplexed detection capabilities, focusing on changes in optical properties when the analyte interacts with the recognition element [19]. Piezoelectric biosensors measure changes in resonance frequency that occur due to the mass of the crystal and the immobilized biological material when an external alternating electrical field is applied [20].

The rapid detection of biological pathogens is crucial in preventing the spread of diseases and infections [21]. Biosensors are extensively used in medical diagnostics, offering specific, sensitive, rapid, and reproducible results compared to traditional methods such as biochemical assays and immunoassays [22]. Their portability and suitability for point-of-care testing make them invaluable in clinical settings [23]. Advances in nanotechnology have further enhanced the performance of biosensors by improving the preparation of biointerfaces, biocompatibility, and resistance to nonspecific adsorption [24], [25].

Point-of-care testing (POCT) is a vital application of biosensors in infection diagnosis, enabling diagnostic tests to be performed near the patient for quick results and more effective treatment [26]. Early and precise diagnoses are crucial for accurately determining the causes and nature of diseases. The shift towards early detection strategies, such as in COVID-19 cases, highlights the importance of non-invasive diagnostic methods like salivary diagnostics, which provide a cost-effective platform for rapid detection and potentially improve patient survival rates [27], [28], [29].

Biosensors are categorized based on their specific applications and mechanisms:

1. Immunosensors: These rely on the specific interactions between antibodies and antigens. They are used for continuous monitoring through point-of-care devices, providing low-cost, fully automated, portable, fast-response, highly sensitive, accurate, and precise measurements. They are employed in clinical diagnosis and monitoring of biomarkers, hormones, pathogenic bacteria, viruses, and toxins [30], [31], [32].

TABLE 1. Benefits and limits of each biosensor type.

BIOSENSOR TYPE	BENEFITS	LIMITS	APPLICATIONS
IMMUNOSENSORS	- High sensitivity and specificity - Fast response time - Portability and ease of use - Low cost in point-of-care setups	- Complex production - Limited shelf life - Costly reagents - Potential interference from sample matrix	- Biomarker detection - Hormone monitoring - Pathogen detection (bacteria, viruses, toxins) - Environmental monitoring
IMMUNOLOGICAL BIOSENSORS	High sensitivity, specificity	Complex production, potential for limited shelf life, susceptibility to sample matrix interference	Detection of viral antigens in air, useful for biomarker detection and pathogen identification
ENZYMATIC BIOSENSORS	- Excellent selectivity - Wide range of analytes can be detected - Versatility in applications - Rapid response time	- Sensitivity to environmental conditions - Limited stability in some cases - Susceptible to enzyme inhibition - Complexity in enzyme immobilization	- Glucose monitoring (diabetes) - Bioprocess monitoring - Food industry (food quality testing) - Environmental monitoring
DNA BIOSENSORS (GENOSENSORS)	High specificity for viral sequences, stability - Relatively simple design - Ability to detect multiple pathogens	- Susceptibility to false positives/negatives, - Technical expertise required for operation - Sensitivity to contaminants - Costly instrumentation	- Pathogen identification (viruses, bacteria) - Forensic analysis - Pharmacogenomics (drug testing)
WHOLE-CELLS	High selectivity for target organisms	Sensitivity to environmental factors	Environmental monitoring (toxins, pollutants)
BIOSENSORS	- Simplicity in cell recognition - Potential for real-time monitoring - Reduced need for specific reagents	- Limited specificity in some cases - Complexity in sensor preparation - Potential for nonspecific interactions	- Biomedical diagnostics (infections, diseases) - Bioremediation (waste treatment) - Industrial applications (food safety, pharmaceuticals)
OPTICAL BIOSENSORS	Multiplexed detection, measurement of optical properties	Equipment complexity, cost, susceptibility to sample matrix interference	Detection of viral particles in the air, analysis of optical properties during viral interaction
PIEZOELECTRIC BIOSENSORS	Detection based on resonance frequency changes	Sensitivity to environmental factors, potential nonspecific interactions	Monitoring resonance frequency due to viral particle accumulation
IMPEDANCE BIOSENSORS	High sensitivity, real-time monitoring, label-free detection	Complex interpretation, specificity challenges	Virus detection, real-time surveillance in hospitals, public spaces, integration into air quality systems

2. Enzymatic Biosensors: These utilize the catalytic properties of enzymes to achieve excellent selectivity for targeted substrates. These biosensors generate electrochemical, optical, or piezoelectric signals correlated with the concentration of the analyte, finding wide applications in point-of-care and clinical settings [33], [34], [35].

3. DNA Biosensors (Genosensors): DNA biosensors use the stability and specificity of DNA to diagnose diseases. By immobilizing DNA or RNA probes on a transducer surface, these biosensors detect complementary target sequences through hybridization, used extensively in clinical applications to detect diseases and pathogens [36], [37].

4. Whole-Cell Biosensors: These use surface antigens on cell envelopes as recognition elements. Despite the challenges posed by the larger size of microorganisms, these biosensors offer high selectivity and sensitivity, making them potential tools in biomedical diagnostics [38].

5. Immunological Biosensors: Advanced devices designed to detect and analyze biological substances by harnessing immune-related interactions. They use antibodies, antigens, or immune cells as recognition elements, providing insights into complex biological interactions and contributing to research, clinical diagnostics, and environmental monitoring [39].

6. Optical Biosensors: These detect and analyze biological compounds through light interactions with the sensor's surface. They allow for multiplexed detection and are crucial in various applications from biomedical diagnostics to food safety monitoring [40].

7. Piezoelectric Biosensors: These detect biological substances by measuring mechanical changes, such as alterations in resonance frequencies due to the binding of target molecules to their surfaces. They are used in disease diagnosis and environmental monitoring [41].

8. Impedance Biosensors: These measure changes in electrical properties, particularly impedance, caused by interactions between the sensor's surface and target molecules. They provide label-free detection and are used in healthcare, environmental monitoring, and research [42].

In conclusion, impedance biosensors offer a promising avenue for detecting airborne viruses, providing real-time monitoring and high sensitivity. However, ensuring specificity and integrating these sensors effectively into existing air quality monitoring systems or infrastructure remains a focus for optimization and practical deployment.

III. SENSOR ARCHITECTURE

In the field of biosensing technology, Silicon Nanowire Field-Effect Transistor (SiNW-FET) biosensors are emerging as exceptionally promising tools for the detection and analysis of biomolecules at the nanoscale. These sensors leverage the distinctive properties of silicon nanowires to achieve highly sensitive and selective detection, proving to be invaluable in areas such as medical diagnostics, environmental monitoring, and pharmaceutical research.

Central to the SiNW-FET biosensor is its complex architecture, meticulously designed to accurately detect target biomolecules. The sensor features a silicon nanowire as the sensing element, which is functionalized with specific receptors (such as immobilized antibodies) that can bind to viruses. This binding induces changes in the electrical properties of the nanowire, which are then converted into an electrical signal. However, the signals produced by the SiNW-FET biosensor are typically very weak, necessitating the inclusion of an amplifier within the sensor's architecture. This amplifier is crucial for enhancing the signal-to-noise ratio (SNR), thus boosting the sensitivity and reliability of the biosensor's output. The SNR was evaluated through detailed simulations using COMSOL and MATLAB. The proposed sensor achieved a signal-to-noise ratio of approximately 70 dB. This high SNR indicates a strong ability to differentiate the signal induced by antibody-antigen interactions from background noise. It also allows the SiNW-FET biosensor to function effectively in real-world settings, where external noise and interference could otherwise compromise signal integrity. Low-pass filter is used to remove high-frequency noise from the sensor signal. Environmental factors such as electromagnetic interference or fluctuations in ambient conditions often introduce high-frequency noise. By applying a low-pass filter, the sensor data retains the relevant low-frequency components that correspond to the impedance changes caused by antibody-antigen interactions, while eliminating unwanted high-frequency noise. By amplifying weak signals and reducing unwanted noise, the biosensor delivers robust performance, making it suitable for a broad array of applications.

The use of a folded-cascade operational amplifier in the sensor's architecture plays a crucial role in amplifying weak signals generated by the nanowire while effectively reducing noise. This design ensures that the signal remains strong relative to any background noise. By carefully adjusting the size and spacing of the electrodes at the nanoscale, the sensor maximizes the interaction between the antibodies and antigens, thereby enhancing the signal strength. The low pass filter was applied in the signal processing stage to
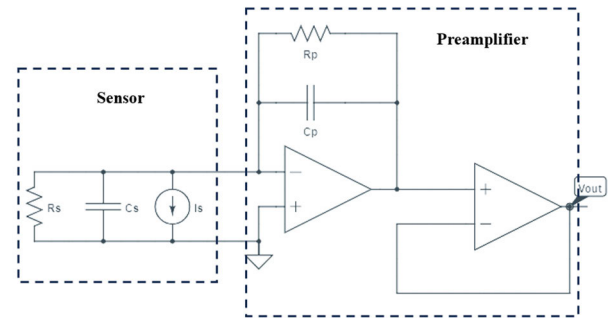

FIGURE 1. Complete sensor architecture.

minimize external interference and environmental noise. This helps maintain a high SNR by ensuring that only relevant signals are amplified and processed. Additionally, the use of high-quality materials with excellent electrical properties reduces inherent noise within the sensor, contributing to a higher SNR. The architecture of this sensor aims to provide a continuous monitoring system characterized by low power consumption and a compact design. The immobilized antibodies on the sensor generate minuscule charge signals, which require a specialized amplifier for processing. Figure 1 depicts the preamplifier scheme integrated with the SiNW-FET sensor, illustrating how this component enhances the sensor's overall functionality.

For operations in the low-frequency range of 10 Hz to 10 kHz, the architecture is optimized to reduce noise, ensure lower power consumption, and enhance charge sensitivity. The Operational Amplifier (OA) within the preamplifier block features a folded-cascade structure, which helps maintain low-frequency operation and utilizes long-channel cascaded MOSFETs in the gain stage to achieve high performance.

The sensor's design incorporates a specific circuit developed for the impedimetric sensing of biomolecules. This setup effectively shapes the sensor's frequency response and provides a reliable readout method for SiNW-FET sensors. The FET is precisely controlled by applying constant DC voltages, while a subtle sinusoidal AC signal is sent to the gate electrode of the FET to fine-tune its operational state.

An elaborate equivalent circuit model serves as the behavioral framework for the SiNW-FET, employing a Level 9 long-channel pMOS transistor (with a width of 320 nm and a length of 12 μm). This model accounts for factors such as the geometries of the drain and source capacitances and the effect of solution conductivity on frequency domain measurements. Figure 2 presents the equivalent small-signal model of this sensor, highlighting the input current (Iin), which feeds into the preamplifier block, illustrating the detailed interactions within the sensor's architecture.

The preamplifier is connected to an input capacitance (Cp), which ranges from 1 to 10 nF as shown in Figure 1. The value of this capacitance is calculated using Equation 1:
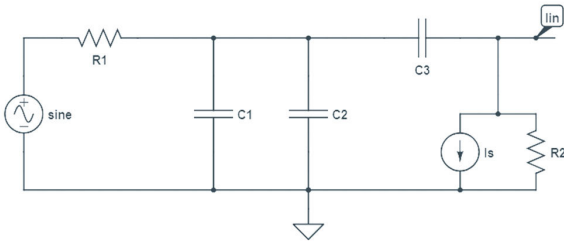
$$C_p = (A_v + 1)C_f \approx A_v C_f \tag{1}$$

FIGURE 2. Equivalent circuit of the SiNW-FET sensor.

Here, Cf represents the feedback capacitance and Av is the open-loop voltage gain of the Operational Amplifier (OA). This calculation is reasonable because the voltage gain Av is significantly greater than 1.

When the sensor is in a state where the receptor is bound, the SiNW-FET sensor generates an output current, I_in. This small AC signal from the current source enters the preamplifier. To prevent any loss of the charge signal, it is crucial that the condition Cp ≫ Cs is met, hence the Cs capacitor is set to a few picofarads.

The transfer function, H(s), is described in Equation 2, and the 3-dB cut-off frequency, ω_3-dB, is defined in Equation 3:

$$H(s) = \frac{V_{out}(s)}{I_{in}(s)} = -\frac{R_p}{1 + sR_pC_p} \quad (2)$$

$$\omega_{3-db} = \frac{1}{R_fC_f} \quad (3)$$

Using these equations, the output voltage in the time domain, V_out(t), is computed as follows:

$$V_{out}(t) = -\frac{1}{C_p}\int I_{in}(t)\,dt + V_{out_{init}}$$

$$V_{out}(t) = -\frac{\Delta Q}{C_p} + + V_{out_{init}} \quad (4)$$

In this formula, $V_{out_{init}}$ represents the initial output voltage, and ΔQ denotes the charge sensitivity of the charge amplifier, which is approximately 1 volt per Cp. These parameters enable the preamplifier to operate effectively in the low-frequency regime, where ω_{3-dB} is just a few hertz. The Rp resistor is about 100 GΩ, achieved using a biased active device. The OA is designed to provide a high dynamic output resistance in alignment with the high resistance value of Rp, as depicted in Figure 3.

The operational amplifier (OA) employs a two-stage amplification setup arranged in a folded-cascade configuration, powered by a 1.1 V supply. The initial stage utilizes a differential amplifier, while the second stage incorporates a common gate amplifier (CGA) configuration to produce a single-ended output voltage, which is then buffered by a voltage buffer. Additionally, a step-down current mirror paired with an 80 nA constant current source is used for circuit biasing, enhancing the match with a specific transducer and controlling the overall conversion gain to prevent voltage saturation.

The design incorporates a substantial pseudo-resistance, as shown in Figure 3, achieved by using long-channel cascaded MOSFETs in the gain stage, which totals 164.80 GΩ (highlighted in green). These MOSFETs have a channel length of 0.8 μm, contrasting sharply with 80 nm for other MOSFETs. This large pseudo-resistance functions similarly to Rf in a charge amplifier setup, influencing the primary 3-dB frequency of the OA, allowing the preamplifier to operate effectively at lower frequencies without the need for large off-chip passive resistances.

The circuit showcases a composite cascade structure where the four input transistors are organized in a way that transistors C and D, which have aspect ratios 12 times that of transistors A and B, are biased in the deep subthreshold region (weak inversion). This configuration reduces the DC current required for the input differential stage, lowering overall power consumption and reducing harmonic distortion compared to operation in the strong inversion region.

OA specifications include a DC open-loop gain (Av) of 58.4 dB with a unity-gain bandwidth of 2.75 MHz. The primary 3-dB pole, ωp1, is set at 6.71 kHz, situated within the range where the open-loop gain remains above 0 dB. There is also a second pole, ωp2, at 5.88 MHz, located outside the OA's effective amplification range. Both poles are positioned in the left half of the pole-zero plane, with ωp2 being notably higher than ωp1. This arrangement ensures a phase margin of 53°, providing stable feedback and minimizing the need for additional compensation to control voltage signal oscillation.

$$|A_{op}| \approx \frac{A_v}{\sqrt{\left(1 + \frac{\omega^2}{\omega_{p1}^2}\right)}} \gg 1 \quad (5)$$

This preamplifier incorporates the OA with the suggested design, featuring an open-loop gain. |Aop| ≫ 1, we have:

$$\frac{V_{out}(s)}{I_{in}(s)} = -\frac{R_p}{1 + sR_pC_p} \quad (6)$$

which corresponds to equation (2) stated for an ideal OA.

IV. SENSOR DESIGN

The simulation of an impedance spectroscopy sensor was conducted using the Finite Element Analysis (FEA) multiphysics software COMSOL. Specifically, the AC-DC module within COMSOL was used to model the electrical response of the sensor, introduce bioselective materials (antigens) to the electrodes, and calculate the impedance changes resulting from the addition of biological target elements (antibodies/IgG).

This simulation employed a nanoscale damascene process that involved patterning a dielectric material (SiO2), filling the pattern with metal electrodes (such as copper), and then planarizing the structure using chemical mechanical planarization (CMP). Figure 1 provides an overview of the sensor configuration used in this study. The electrodes were specified by their width (A), length (F), and spacing (B). Below the electrodes, an insulating layer of SiO2 (D) was
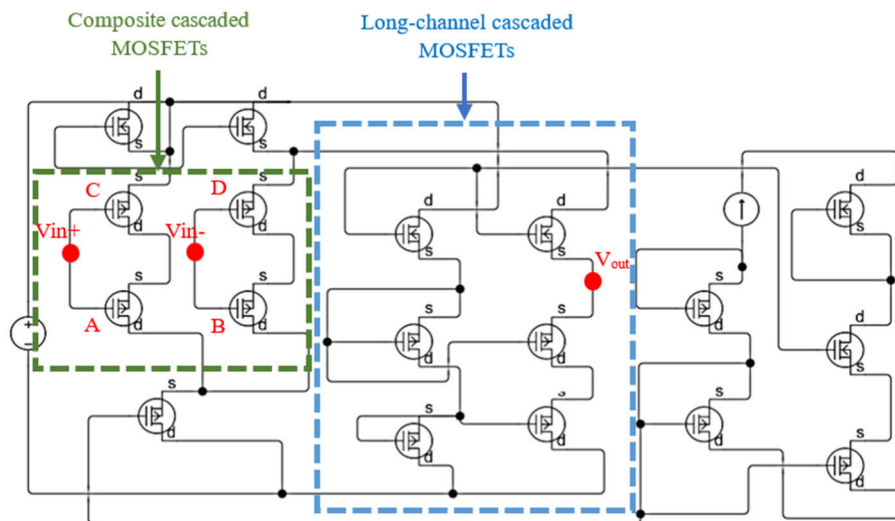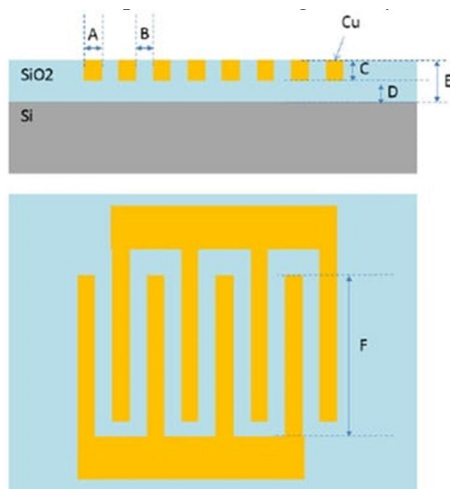
FIGURE 3. Operational amplifier schematic.

placed, with the total thickness of this insulator noted as E. The specific dimensions used in the simulations are detailed in Figure 4, which depicts the overall geometry of the sensor.

(A=60 nm) Width of finger, (B=60) Spacing between fingers, (C=100 nm) Thickness of fingers, (D=80 nm) Amount of insulator below fingers, (E=280 nm) Total thickness of insulator, and (F=1500 nm) Length of each finger

FIGURE 4. Configuration of the electrode sensor.

In the COMSOL simulations, the sensor's electrodes functioned as the capacitive components within an RC circuit. This model allowed for the detailed examination and manipulation of the electrodes' geometry to study changes in electrical impedance, especially in relation to antibody-antigen interactions. For the simulation, protein-based antigens were applied to the electrode surface and anchored with a thin attachment layer, followed by the addition of an antibody (IgG) layer (as shown in Figure 5). This setup replicates a typical biosensing technique where antibodies in the bloodstream interact with the sensor, signaling an immune response

to a pathogen. By using this method, even minor changes in the amount of antibodies bound to antigens on the electrode surface were expected to result in significant impedance changes.

The antigen used in our SiNW-FET biosensor is a protein-based antigen with dimensions of 60×80 nm. This protein-based antigen is chosen for its ability to specifically interact with the immobilized antibodies on the silicon nanowire, leading to detectable changes in the sensor's impedance.

The antibody employed in this study is Immunoglobulin G (IgG), with dimensions of $60 \times 60 \times 80$ nm. The IgG antibodies are functionalized on the silicon nanowire surface to ensure specific binding with the target antigens. The relative permittivity (epsilon) of the IgG antibodies is 10, and their electric conductivity (sigma) is 0.825 μS/m. These properties are essential for creating a sensitive and specific biosensing environment. When the antigens bind to these antibodies, they cause measurable changes in the electrical properties of the nanowire, which the sensor detects as impedance variations.
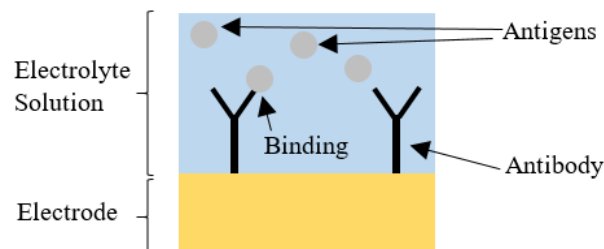

FIGURE 5. Binding principle of antigens with antibody.

Table 2 details the dimensions and characteristics of the antigens and antibodies used in the simulations [43], [44].

In these models, the protein antigens were represented as a thin layer coating the electrodes, while the IgG antibodies were shown as a series of blocks attached to this protein layer. By adjusting the number of blocks in the array, the simulation could vary the overall concentration or amount of antigens and antibodies binding to the electrodes, effectively modeling their interaction dynamics.

TABLE 2. Characteristics of antigen and antibody.

ANTIBODY DIMENSION	60 X 60 X 80 NM
PROTEIN	60 x 80 nm
RELATIVE PERMITTIVITY (EPSILON)	10
ELECTRIC CONDUCTIVITY (SIGMA)	0.825µ S/m

The Nyquist plot, which compares the imaginary component of impedance (Z) with its real component, was used to visually represent changes in impedance when protein or IgG was added to the electrode surface. The core concept of this analysis is that increasing the dielectric material on the electrode would raise the resistance (and possibly the capacitance), leading to a larger semi-circle diameter on the plot, which indicates a higher absolute value of impedance.

The evaluation of the proposed sensor architecture is ensured by the following performance metric.

Accuracy is a measure of the overall correctness of a diagnostic test. It is the proportion of true results (both true positives and true negatives) among the total number of cases examined. Accuracy provides a general sense of how well the sensor performs across all tested samples. It is calculated using the equation 7.

$$Accuracy = \frac{Number\ of\ Correct\ Prediction}{Total\ Number\ of\ Prediction} \quad (7)$$

A higher accuracy indicates that the sensor correctly identifies both the presence and absence of the target virus in the majority of cases.

Sensitivity, also known as the true positive rate or recall, measures the proportion of actual positives that are correctly identified by the sensor. It indicates how well the sensor detects the presence of the virus when it is indeed present. Sensitivity is particularly important in ensuring that cases of infection are not missed. It is calculated using the equation.

$$Sensitivity = \frac{TP}{TP + FN} \quad (8)$$

High sensitivity means the sensor is effective at detecting the virus when it is present, minimizing the likelihood of false negatives.

Specificity, also known as the true negative rate, measures the proportion of actual negatives that are correctly identified by the sensor. It indicates how well the sensor identifies the absence of the virus when it is not present. Specificity is crucial for ensuring that non-infected cases are not falsely identified as infected. It is calculated using the equation 9.

$$Specificity = \frac{TN}{TN + FP} \quad (9)$$

High specificity means the sensor is effective at confirming the absence of the virus, reducing the occurrence of false positives.

Since the study is currently based on a simulated version of the SiNW-FET biosensor, the classification process involved creating a set of simulated samples with known statuses, representing both virus-positive and virus-negative cases. Each simulated sample was tested using the SiNW-FET biosensor simulation model, and the output indicating whether a sample was positive or negative for the virus was recorded. The simulated sensor's results were compared with the known true status of each sample to determine the classification.

V. SIMULATION: RESULTS AND DISCUSSION
COMSOL and MATLAB were utilized to simulate the sensor, confirming the initial findings presented in this paper. The simulations began by exploring the relationship between impedance and virus detection, and subsequently examined how design modifications affect impedance readings at different frequencies. Nyquist plots were used as a visual tool to demonstrate impedance changes under various conditions, with the expectation that impedance would increase with higher concentrations of protein.

A. ESTABLISHING THE CONNECTION BETWEEN IMPEDANCE AND PROTEIN DETECTION
Initially, COMSOL simulated three different scenarios for the nanoscale sensor. The first scenario featured bare electrodes without any protein-based antigens or IgG on the copper electrodes. In the second scenario, an antigen coating was applied to the copper electrodes, but without any IgG binding. The third scenario explored the binding of IgG to the antigen-coated layer. Figure 6 shows the simulated impedance responses for each scenario. As expected, the addition of protein materials to the sensor electrodes resulted in an increase in impedance. Moreover, adding a small amount of antibody (IgG) on top of the antigen layer led to a slight, though not significant, change in impedance. However, a nearly complete binding of antigen to antibody caused a substantial increase in impedance.

B. EXPLORING SENSOR DIMENSIONS
The study also investigated the impact of electrode dimensions on impedance, specifically changes in electrode width (A) and the spacing between electrodes (B). Nyquist plots were generated from these simulations, maintaining a consistent quantity of antibody and antigen throughout the tests.

Figure 6 presents a Nyquist plot featuring four curves that demonstrate variations in impedance under different conditions, reflecting the biosensor's responses. The spacing between these curves and their initial positions on the imaginary axis (Im(Z)) help to illustrate the level of binding and the biosensor's specificity to various antigens. Typically, a higher starting point on Im(Z) indicates stronger and more specific binding, whereas a lower starting point suggests weaker or nonspecific interactions.
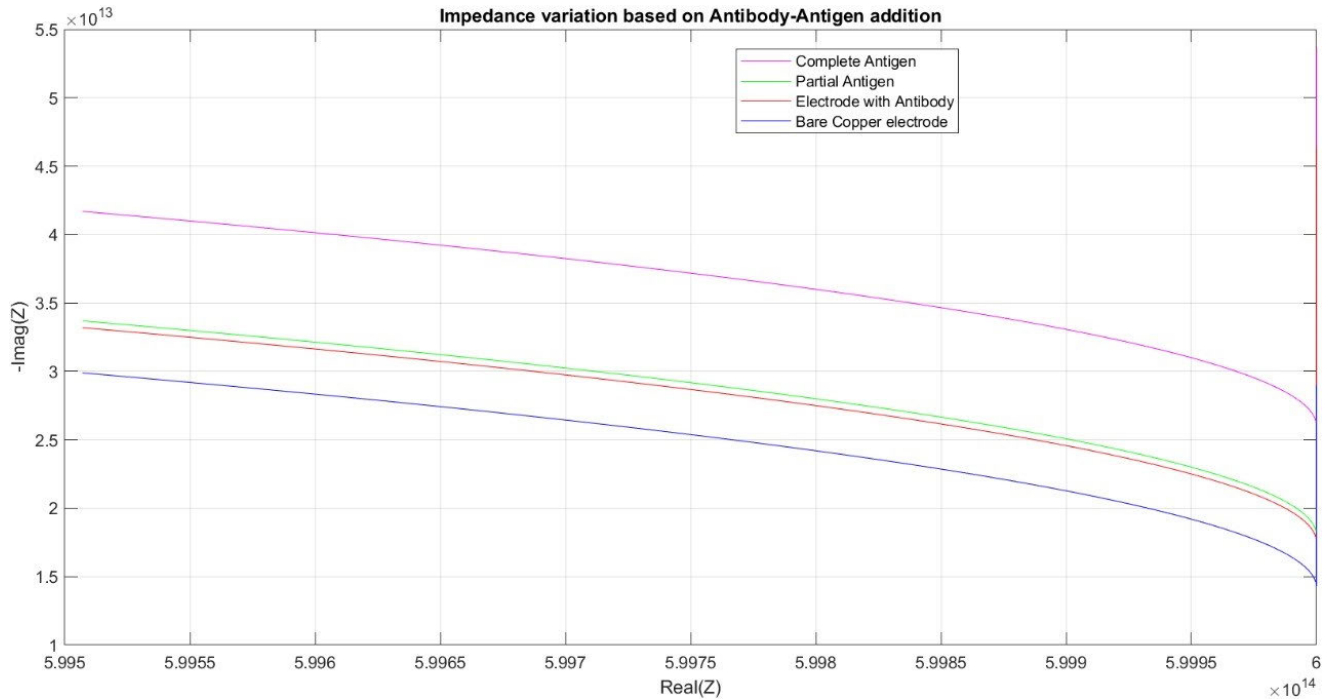
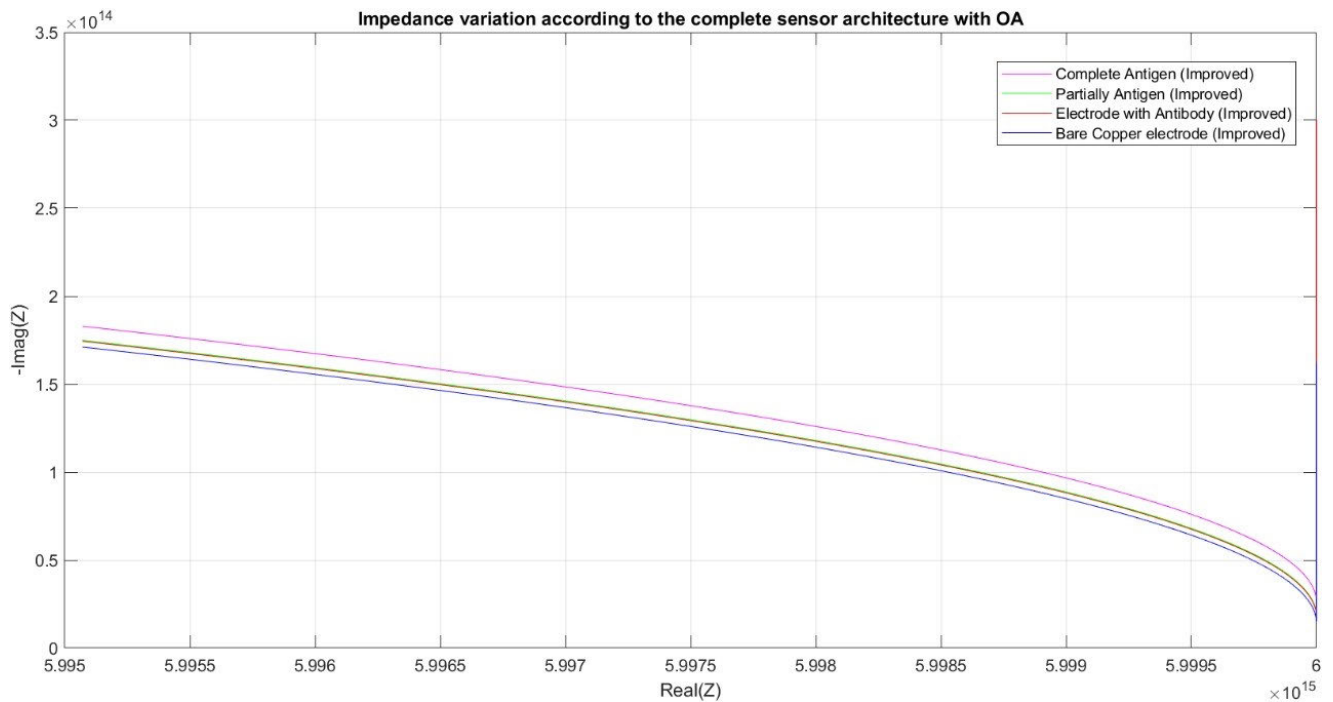**FIGURE 6.** Effect of antibody-antigen on impedance.

FIGURE 7. Effect of antibody-antigen on the impedance of the complete sensor architecture.

The "Bare Copper Electrode" curve serves as the baseline, showing the impedance without any modifications or interactions with antigens or antibodies. This curve provides a reference point for comparing the effects of modifications on the electrodes. The "Electrode with Antibody" curve represents the impedance when antibodies, which can specifically bind to antigens, are attached to the electrode. This demonstrates how the attachment of antibodies influences the overall impedance of the biosensor. The "Partial Antigen" curve reflects the impedance when a partially specific antigen
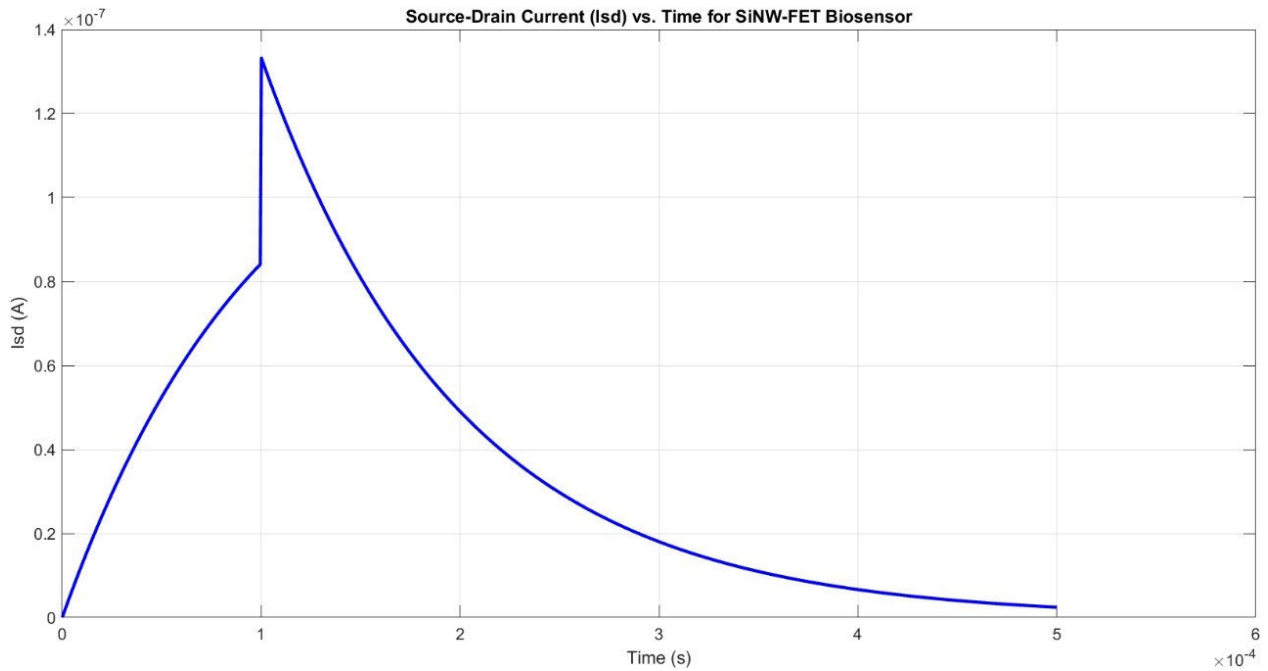
FIGURE 8. The proposed SiNW-FET biosensor response.
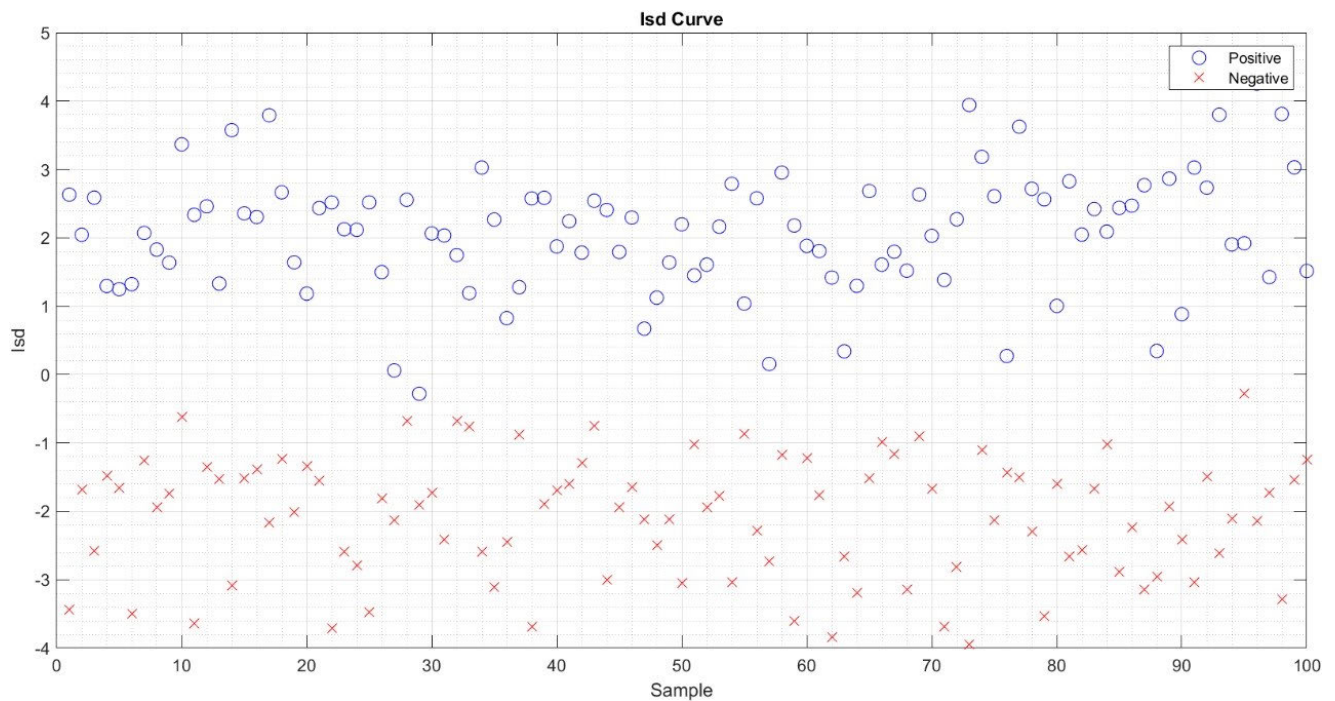
FIGURE 9. Isd current distribution.

is present, indicating incomplete binding with the attached antibodies and the resultant change in impedance. The curve labeled "Complete Antigen" displays the impedance when a fully specific antigen is present, leading to complete binding with the attached antibodies and showing the highest

impedance change, which underscores the biosensor's specificity and sensitivity to the target antigen.

Overall, the Nyquist plot offers valuable insights into the biosensor's ability to detect specific antigens, with the "Complete Antigen" curve showing the most significant change

TABLE 3. A comparison based structure and performance.

Criteria	Proposed Work	Yang, X., et al. [45] (2019)	Yao, X., et al. [46] (2021)	Sengupta, J., et al. [47] (2021)
Sensor Structure	SiNW-FET with folded-cascade amplifier	SiNW-FET with basic amplifier	Carbon Nanotube FET (CNT-FET)	Graphene FET (G-FET)
Electrode Material	Silicon	Silicon	Carbon nanotubes	Graphene
Functionalization	Antibody functionalization on nanowires	Antibody functionalization on nanowires	Antibody functionalization on nanotubes	Antibody functionalization on graphene
Signal Amplification	Folded-cascade operational amplifier	Simple operational amplifier	No additional amplification	Differential amplifier
Accuracy	92%	85%	80%	88%
Sensitivity	85%	78%	75%	82%
Specificity	99%	90%	88%	95%
Signal-to-Noise Ratio (SNR)	70 dB	60 dB	55 dB	65 dB
Environmental Stability	High, with advanced filtering techniques	Moderate, basic filtering	Low, minimal filtering	High, with differential filtering
Power Consumption	Low	Moderate	High	Low
Real-time Monitoring	Yes	Yes	No	Yes

in impedance, followed by the ''Partial Antigen'' and ''Electrode with Antibody'' curves, and finally the ''Bare Copper Electrode'' curve as the baseline reference.

Figure 7 displays the impedance output when the sensor is coupled with the proposed Operational Amplifier (OA). The curves associated with the operational amplifier reveal more significant shifts on the Nyquist plot in response to impedance changes, highlighting increased sensitivity. These plots also show reduced fluctuation or noise, which enhances the precision of the impedance measurements.

The incorporation of the proposed OA, as discussed in Section III, offers several benefits:
- Improved Sensitivity: The amplifier boosts the impedance signal, thereby enhancing the biosensor's ability to detect subtle changes in impedance.
- Noise Reduction: The amplifier minimizes electrical noise, which improves the accuracy of impedance measurements.
- Increased Dynamic Range: The amplifier extends the range of impedance values that can be measured, allowing for more precise detection across a wider range.

C. PERFORMANCE EVALUATION

Figure 8 presents the Isd (source-drain current) versus Time curve for a SiNW-FET biosensor, which directly indicates the sensor's accuracy in detecting viruses. The curve demonstrates a decline in the source-drain current over time, likely due to the binding of target molecules to the surface of the SiNW. This interaction depletes the channel and diminishes the current flow, with the rate of this decline used to gauge the concentration of target molecules in a sample.

The Isd vs. Time curve essentially captures the electrical behavior of the SiNW-FET biosensor as it responds to applied voltages and the presence of charges on the sensor surface. Evaluating the accuracy of virus detection involves comparing the biosensor's response to known virus samples (true positives) and non-virus samples (true negatives) across

various concentrations. This comparison facilitates statistical analyses including sensitivity, specificity, positive predictive value, and negative predictive value.

To assess the proposed sensor design, a simulated dataset containing the Isd current and classification labels is analyzed. Figure 9 displays the classification results, where each point on the x-axis represents a sample from the Isd dataset, and the y-axis shows the corresponding Isd values. Isd is a measure of the current flowing between the source and drain terminals of a device, commonly used in semiconductor characterization. Data points identified as positive are marked with blue circles. Within this simulated data, positive class points denote true positives (TP) and false positives (FP) according to the set threshold. Similarly, data points labeled as negative are shown with red crosses, representing true negatives (TN) and false negatives (FN). Figure 9 illustrates the distribution of Isd values across positive and negative classes, providing insights into the performance of the sensor.

The proposed sensor design achieved an accuracy of approximately 92%, calculated using Equation 7, a sensitivity of about 85%, determined using Equation 8, and a specificity of roughly 99%, based on Equation 9.

The comparison table highlights the unique aspects and improvements of the proposed SiNW-FET biosensor compared to similar works in the literature. Key differentiators include the use of a folded-cascade operational amplifier for enhanced signal amplification, advanced filtering techniques for environmental stability, and superior performance metrics such as higher accuracy, sensitivity, and specificity. These enhancements demonstrate the novelty and effectiveness of the proposed biosensor in real-time, non-invasive healthcare monitoring applications.

VI. CONCLUSION

This study has successfully demonstrated the design, simulation, and verification of a novel SiNW-FET biosensor for healthcare applications, focusing on the detection of viral

infections through impedance measurements. The utilization of COMSOL/MATLAB simulations enabled a detailed analysis of how electrode functionalization with antibodies and changes in electrode dimensions influence the sensor's sensitivity and specificity. The proposed sensor achieved impressive performance metrics, with an accuracy of approximately 92%, sensitivity around 85%, and specificity near 99%. These results highlight the sensor's potential for real-time, non-invasive monitoring of viral biomarkers, offering a significant advancement over traditional methods which often involve cumbersome and expensive equipment.

Moreover, the sensor's ability to operate effectively in a home setting addresses a critical need for continuous health monitoring, potentially reducing the frequency of hospital visits and allowing for earlier detection and intervention in viral infections. The high specificity and sensitivity also indicate that the sensor could be adapted for the detection of various other biomolecules, broadening its applicability in the medical field.

Future work will focus on further optimization of the sensor design to enhance its operational stability and to test its effectiveness in a wider range of environmental conditions and across different types of viral and cellular biomarkers. This ongoing development could pave the way for a new generation of home-based diagnostic tools, fundamentally changing how patients manage their health and interact with the healthcare system.

REFERENCES

[1] I. Turcan and M. A. Olariu, "Dielectrophoretic manipulation of cancer cells and their electrical characterization," *ACS Combinat. Sci.*, vol. 22, no. 11, pp. 554–578, Nov. 2020.

[2] J. Chen, Z. Fang, J. Liu, and L. Zeng, "A simple and rapid biosensor for ochratoxin a based on a structure-switching signaling aptamer," *Food Control*, vol. 25, no. 2, pp. 555–560, Jun. 2012.

[3] J. N. Anker, W. P. Hall, O. Lyandres, N. C. Shah, J. Zhao, and R. P. Van Duyne, "Biosensing with plasmonic nanosensors," *Nature Mater.*, vol. 7, no. 6, pp. 442–453, Jun. 2008.

[4] X. Zeng, Z. Shen, and R. Mernaugh, "Recombinant antibodies and their use in biosensors," *Anal. Bioanal. Chem.*, vol. 402, no. 10, pp. 3027–3038, Apr. 2012.

[5] H. Yu, O. Alkhamis, J. Canoura, Y. Liu, and Y. Xiao, "Advances and challenges in small-molecule DNA aptamer isolation, characterization, and sensor development," *Angew. Chem. Int. Ed.*, vol. 60, no. 31, pp. 16800–16823, 2021.

[6] H.-J. Jang, J. Ahn, M.-G. Kim, Y.-B. Shin, M. Jeun, W.-J. Cho, and K. H. Lee, "Electrical signaling of enzyme-linked immunosorbent assays with an ion-sensitive field-effect transistor," *Biosensors Bioelectron.*, vol. 64, pp. 318–323, Feb. 2015.

[7] J. Ahn, T. H. Lee, T. Li, K. Heo, S. Hong, J. Ko, Y. Kim, Y.-B. Shin, and M.-G. Kim, "Electrical immunosensor based on a submicron-gap interdigitated electrode and gold enhancement," *Biosensors Bioelectron.*, vol. 26, no. 12, pp. 4690–4696, Aug. 2011.

[8] H. S. Magar, R. Y. A. Hassan, and A. Mulchandani, "Electrochemical impedance spectroscopy (EIS): Principles, construction, and biosensing applications," *Sensors*, vol. 21, no. 19, p. 6578, Oct. 2021.

[9] C. Honrado, P. Bisegna, N. S. Swami, and F. Caselli, "Single-cell microfluidic impedance cytometry: From raw signals to cell phenotypes using data analytics," *Lab Chip*, vol. 21, no. 1, pp. 22–54, 2021.

[10] S. Das, D. Das, S. Maiti, and K. Biswas, "A bioimpedance-based microflow cytometer with compact electronic instrumentation for counting of microparticles," in *Proc. 9th Int. Conf. Sens. Technol. (ICST)*, Dec. 2015, pp. 157–161.

[11] W. H. Grover, "Interdigitated array electrode sensors: Their design, efficiency, and applications," Ph.D. dissertation, Dept. Chem., Univ. Tennessee, Knoxville, TN, USA, 1999.

[12] M. Abdallah, "Design, simulation, and development of a BioSensor for viruses detection using FPGA," *IEEE J. Translational Eng. Health Med.*, vol. 9, pp. 1–6, 2021.

[13] J. A. Goode, J. V. H. Rushworth, and P. A. Millner, "Biosensor regeneration: A review of common techniques and outcomes," *Langmuir*, vol. 31, no. 23, pp. 6267–6276, Jun. 2015.

[14] F. Yang, Y. Ma, S. G. Stanciu, and A. Wu, "Transduction process-based classification of biosensors," in *Nanobiosensors: From Design to Applications*, 1st ed. Wiley-VCH, Jun. 2020, pp. 23–44.

[15] J. Ding and W. Qin, "Recent advances in potentiometric biosensors," *Trends Anal. Chem.*, vol. 124, Mar. 2020, Art. no. 115803.

[16] N. Labban, L. Hughes, M. Wayu, J. Pollock, and M. Leopold, "MON-182 adaptable amperometric biosensor platforms for the diagnosis of endocrine disorders," *J. Endocrine Soc.*, vol. 3, pp. 18–31, Apr. 2019.

[17] E. B. Aydın, "Highly sensitive impedimetric immunosensor for determination of interleukin 6 as a cancer biomarker by using conjugated polymer containing epoxy side groups modified disposable ITO electrode," *Talanta*, vol. 215, Aug. 2020, Art. no. 120909.

[18] Y. Zhang, Y. Zhu, S. Zheng, L. Zhang, X. Shi, J. He, X. Chou, and Z.-S. Wu, "Ink formulation, scalable applications and challenging perspectives of screen printing for emerging printed microelectronics," *J. Energy Chem.*, vol. 63, pp. 498–513, Dec. 2021.

[19] H. Altug, S.-H. Oh, S. A. Maier, and J. Homola, "Advances and applications of nanophotonic biosensors," *Nature Nanotechnol.*, vol. 17, no. 1, pp. 5–16, Jan. 2022.

[20] Y. Su, W. Li, L. Yuan, C. Chen, H. Pan, G. Xie, G. Conta, S. Ferrier, X. Zhao, G. Chen, H. Tai, Y. Jiang, and J. Chen, "Piezoelectric fiber composites with polydopamine interfacial layer for self-powered wearable biomonitoring," *Nano Energy*, vol. 89, Nov. 2021, Art. no. 106321.

[21] A. A. Ansari and B. D. Malhotra, "Current progress in organic–inorganic hetero-nano-interfaces based electrochemical biosensors for healthcare monitoring," *Coordination Chem. Rev.*, vol. 452, Feb. 2022, Art. no. 214282.

[22] S. Ramanavicius and A. Ramanavicius, "Development of molecularly imprinted polymer based phase boundaries for sensors design (review)," *Adv. Colloid Interface Sci.*, vol. 305, Jul. 2022, Art. no. 102693.

[23] Z. Li, J. Zhang, Y. Huang, J. Zhai, G. Liao, Z. Wang, and C. Ning, "Development of electroactive materials-based immunosensor towards early-stage cancer detection," *Coordination Chem. Rev.*, vol. 471, Nov. 2022, Art. no. 214723.

[24] W.-C. Lan, T.-S. Huang, Y.-C. Cho, Y.-T. Huang, C. J. Walinski, P.-C. Chiang, M. Rusilin, F.-T. Pai, C.-C. Huang, and M.-S. Huang, "The potential of a nanostructured titanium oxide layer with self-assembled monolayers for biomedical applications: Surface properties and biomechanical behaviors," *Appl. Sci.*, vol. 10, no. 2, p. 590, Jan. 2020.

[25] M. Garhnayak, A. Mahapatra, L. Garhnayak, S. Rath, and A. K. Kar, "Biosensor as quick analytic tool in pandemic!" in *Biosensors for Emerging and Re-Emerging Infectious Diseases*. Amsterdam, The Netherlands: Elsevier, 2022, pp. 169–196.

[26] A. Gopal, L. Yan, S. Kashif, T. Munshi, V. A. L. Roy, N. H. Voelcker, and X. Chen, "Biosensors and point-of-care devices for bacterial detection: Rapid diagnostics informing antibiotic therapy," *Adv. Healthcare Mater.*, vol. 11, no. 3, Feb. 2022, Art. no. 2101546.

[27] D. C. Caixeta, L. R. Paranhos, C. Blumenberg, M. A. Garcia-Júnior, M. Guevara-Vega, E. B. Taveira, M. A. C. Nunes, T. M. Cunha, A. N. G. Jardim, C. Flores-Mir, and R. Sabino-Silva, "Salivary SARS-CoV-2 RNA for diagnosis of COVID-19 patients: A systematic review and meta-analysis of diagnostic accuracy," *Jpn. Dental Sci. Rev.*, vol. 59, pp. 219–238, Dec. 2023.

[28] M. Ben Ayed, A. Massaoudi, and S. A. Alshaya, "Smart recognition COVID-19 system to predict suspicious persons based on face features," *J. Electr. Eng. Technol.*, vol. 16, no. 3, pp. 1601–1606, May 2021.

[29] T. Nguyen, D. Duong Bang, and A. Wolff, "2019 novel coronavirus disease (COVID-19): Paving the road for rapid detection and point-of-care diagnostics," *Micromachines*, vol. 11, no. 3, p. 306, Mar. 2020.

[30] J. Kelch, A. Delaney, F. Kelleher, P. Baker, E. Iwuoha, and E. Dempsey, "Impedimetric and electrochemical evaluation of a new redox active steroid derivative for hormone immunosensing," *Biosensors Bioelectron.*, vol. 150, Feb. 2020, Art. no. 111876.

[31] C. D. C. Santos, P. C. M. Santos, K. L. S. Rocha, R. L. Thomasini, D. B. de Oliveira, D. L. Franco, and L. F. Ferreira, "A new tool for dengue virus diagnosis: Optimization and detection of anti-NS1 antibodies in serum samples by impedimetric transducers," *Microchemical J.*, vol. 154, May 2020, Art. no. 104544.

[32] K. Halicka and J. Cabaj, "Electrospun nanofibers for sensing and biosensing applications—A review," *Int. J. Mol. Sci.*, vol. 22, no. 12, p. 6357, Jun. 2021.

[33] U. Gupta, V. Gupta, R. K. Arun, and N. Chanda, "Recent advances in enzymatic biosensors for point-of-care detection of biomolecules," *Biotechnol. Bioeng.*, vol. 119, no. 12, pp. 3393–3407, Dec. 2022.

[34] I. Rahmawati, Y. Einaga, T. A. Ivandini, and A. Fiorani, "Enzymatic biosensors with electrochemiluminescence transduction," *ChemElectroChem*, vol. 9, no. 12, Jun. 2022, Art. no. e202200175.

[35] R. Bi, X. Ma, K. Miao, P. Ma, and Q. Wang, "Enzymatic biosensor based on dendritic gold nanostructure and enzyme precipitation coating for glucose sensing and detection," *Enzyme Microbial Technol.*, vol. 162, Jan. 2023, Art. no. 110132.

[36] L. Hilda, M. S. Mutlaq, I. Waleed, R. H. Althomali, M. H. Mahdi, S. S. Abdullaev, R. Singh, H. A. Nasser, Y. F. Mustafa, and A. H. R. Alawadi, "Genosensor on-chip paper for point of care detection: A review of biomedical analysis and food safety application," *Talanta*, vol. 268, Feb. 2024, Art. no. 125274.

[37] A. Babaei, A. Pouremamali, N. Rafiee, H. Sohrabi, A. Mokhtarzadeh, and M. de la Guardia, "Genosensors as an alternative diagnostic sensing approaches for specific detection of virus species: A review of common techniques and outcomes," *Trends Anal. Chem.*, vol. 155, Oct. 2022, Art. no. 116686.

[38] Z. Štukovnik and U. Bren, "Development and optimization of an electrochemical-impedimetric biosensor based on whole cells for the detection of active compounds," in *Book of Abstracts, GEHPT and ESS-HPT Green Engineering by High Pressure Technology*. The European Summer School in High Pressure Technology, University of Maribor and Graz University of Technology, Jul. 2022.

[39] X. Ren, H. Ma, T. Zhang, Y. Zhang, T. Yan, B. Du, and Q. Wei, "Sulfur-doped graphene-based immunological biosensing platform for multianalysis of cancer biomarkers," *ACS Appl. Mater. Interfaces*, vol. 9, no. 43, pp. 37637–37644, Nov. 2017.

[40] A. Uniyal, G. Srivastava, A. Pal, S. Taya, and A. Muduli, "Recent advances in optical biosensors for sensing applications: A review," *Plasmonics*, vol. 18, no. 2, pp. 735–750, Apr. 2023.

[41] S. Huang, Y. Gao, Y. Hu, F. Shen, Z. Jin, and Y. Cho, "Recent development of piezoelectric biosensors for physiological signal detection and machine learning assisted cardiovascular disease diagnosis," *RSC Adv.*, vol. 13, no. 42, pp. 29174–29194, 2023.

[42] Y.-S. Chen, C.-H. Huang, P.-C. Pai, J. Seo, and K. F. Lei, "A review on microfluidics-based impedance biosensors," *Biosensors*, vol. 13, no. 1, p. 83, Jan. 2023.

[43] R. Saber, S. Sarkar, P. Gill, B. Nazari, and F. Faridani, "High resolution imaging of IgG and IgM molecules by scanning tunneling microscopy in air condition," *Scientia Iranica*, vol. 18, no. 6, pp. 1643–1646, Dec. 2011.

[44] S. Logeshkumar, L. Lavanya, A. Gupta, and M. Alagappan, "FEM based estimation of biological interaction using a cantilever array sensor," in *Proc. COMSOL*, 2011, pp. 121–129.

[45] X. Yang, Y. Fan, Z. Wu, and C. Liu, "A silicon nanowire array biosensor fabricated by complementary metal oxide semiconductor technique for highly sensitive and selective detection of serum carcinoembryonic antigen," *Micromachines*, vol. 10, no. 11, p. 764, Nov. 2019.

[46] X. Yao, Y. Zhang, W. Jin, Y. Hu, and Y. Cui, "Carbon nanotube field-effect transistor-based chemical and biological sensors," *Sensors*, vol. 21, no. 3, p. 995, Feb. 2021.

[47] J. Sengupta and C. M. Hussain, "Graphene-based field-effect transistor biosensors for the rapid detection and analysis of viruses: A perspective in view of COVID-19," *Carbon Trends*, vol. 2, Jan. 2021, Art. no. 100011.

AHMED HADDED received the master's degree in embedded electronics from the University of Lorraine, France, in 2020. He is currently pursuing the Ph.D. degree with the National School of Engineers of Sfax, Tunisia. He was an Active Researcher with the Embedded Computer Systems Laboratory (CES) and carried out research in the field of intelligent systems and signal processing.

MOSSAAD BEN AYED received the degree in electrical engineering, in 2007, the Ph.D. (Diploma) degree in embedded systems in the field of simulation, in 2013, and the H.D.R. degree in embedded systems, in 2019. In 2007, he was an Active Researcher with the Laboratory of Computer Embedded System (CES), National Engineering School of Sfax, Tunisia (http://ceslab.org/fr/perso.phpid=81). He is currently an Associate Professor with the College of Engineering at Sousse, Tunisia. His research interests include embedded systems, simulation, computer-aided design, emulation, modeling, co-design, and pattern recognition.

SHAYA ABDULLAH ALSHAYA received the bachelor's and master's degrees in Saudi Arabia, USA, and Italy. He has put his knowledge into practicality as an International Entrepreneur and his endeavors include education and research and ICT sector. He is currently an Assistant Professor with the College of Science and Humanities at Al-Ghat, Majmaah University, Riyadh, Saudi Arabia. He is also a member of the National Association of Industrial Technology, the Institute of Electrical Engineers, and the Sloan-C Online Association. He has a wealthy experience as the Head of IT with Majmaah University. His experience as a Researcher, a Consultant, a Project Manager, and an Information Technologist has allowed him to bring his extensive experience of technology planning, training, and implementation to all of the projects he endeavors. The numerous national and international companies that utilize his expertise as a Consultant evidence his success. His wealthy experience, vast knowledge is integral to his vision and future projects.

• • •